Enabling Climate Information Services for Europe

Report

DELIVERABLE 6.5
Report on past and future stream flow estimates coupled to dam flow evaluation and hydropower production potential

Activity:	*WP6 – Energy*
Activity number:	*Task 6.2 - Dams management in hydropower generation in Alpine and Apennines regions*
Deliverable:	*Past and future stream flow estimates coupled to dam flow evaluation and hydropower production potential*
Deliverable number:	*6.5*
Authors:	*Michele BRUNETTI, Claudia SIMOLO - ISAC-CNR; Maurizio MAUGERI - University of Milan; Francesco DALLA VALLE, Giorgio GALEATI, Roberto MANFREN, Lorenzo VERONESE - ENEL*

The work leading to this publication has received funding from the European Union's Seventh Framework Programme (FP7/2007-2013) under grant agreement n° 265240.

Summary

The deliverable aims at evaluating the relationship existing between climate variability (as far as precipitation and temperature are concerned) and the potential productivity of 4 Enel hydropower plants located in the Cordevole river catchment, chosen as a case study. This catchment is located in the upper part of the Piave river catchment, in the eastern Alps.

To capture this relationship, we provided ENEL with a 30-arc-second resolution dataset of monthly temperature and precipitation over the case study area for the past decades and for the future, based on the statistical downscaling of some ENSEMBLES RCMs.

These data were used by ENEL to calibrate and validate their empirical model of plant productivity over the past, and to project it into the future, estimating the productivity evolution under an A1B scenario.

1. Introduction

In the previous deliverable (deliverable 6.4) of this task we produced 30-arc-second resolution monthly precipitation data for past decades over the upper part of the Piave river catchment, reconstructing separately the spatial and the temporal structure of the precipitation field (the former is basically linked to the geographical features of the territory and it can manifest remarkable spatial gradients, the latter is linked to climate variability and change and it is generally characterized by higher spatial coherence).

A Local Weighted Linear Regression (LWLR) of precipitation versus elevation (where stations are weighted based on the similarity of their geographical feature to that of the grid cell) has been used to estimate the climatology (spatial field), and a more simple method (based on an inverse distance weighting procedure with the addition of an angular weight to take into account anisotropy in station spatial distribution) was used to construct the time-dependent anomalies on the same grid-nodes. From the superimposition of the two fields (climatologies and anomalies) we obtained a monthly precipitation data set in absolute values at 30 arc-second resolution.

From a discussion with ENEL, we realised the necessity of providing also temperature data over the same grid to take into account the snow fraction in precipitation amount and the snow melting. So, with the same LWLR (with parameters optimized for temperatures), a monthly high resolution temperature data set was produced too.

These data (provided for the 1951-2010 period) constitute the starting point for the estimation of the relationship existing between climate variability and the potential productivity of the hydropower plants considered in the case study discussed in this report.

2. Description of the procedure to estimate the relationship between climate variability and the potential productivity of an hydropower plant

ENEL has productivity data of the 4 hydropower plants of the Cordevole catchment since 1975. These data were used to calibrate and validate an empirical model for the estimation of the productivity starting from meteorological data.

A rigorous evaluation of the stream flow requires, beside the precipitation amount, an evaluation of the snow melting. To do this, a daily temperature and precipitation dataset would be necessary, but this was not planned within this task and it was not possible to do this additional work because it would need the collection of an adequate number of daily temperature and precipitation series. So, we used a method that allows estimating the snow melting starting from monthly data.

2.1 Snow Water Equivalent estimation

Thanks to the daily temperature series of the dam network of ENEL (5 series), the relationship between the standard deviation of the differences of daily mean temperatures from the corresponding monthly mean and the monthly mean has been evaluated (see table 1) to obtain an estimation of the occurrence of mean daily temperatures above a fixed melting threshold.

This was necessary both to evaluate the snow melt potential and to estimate the fraction of solid and liquid precipitation (snow below 1°C, rain above 1°C)

Monthly mean (°C)	Standard deviation (°C)
-10	3.7
-9	3.7
-8	3.7
-7	3.7
-6	3.7
-5	2.9
-4	2.9
-3	2.4
-2	2.8
-1	2.3
0	2.4
1	2.8
2	3.3
3	3.1
4	2.5
5	2.6
6	2.7
7	2.8
8	2.9
9	2.8
10	2.6
11	2.5
12	2.6
13	2.6
14	2.3
15	2.5
16	2.7
17	2.2
18	2.3
19	2.1
20	2.0

Table 1. Standard deviation of the differences of the daily mean temperatures from the corresponding monthly mean as a function of the monthly mean.

The data of table 1 permit the estimation of the distribution of the daily temperatures around the monthly mean for each point of the domain for which a monthly temperature series has been generated in the first part of the ECLISE Project (see deliverable 6.4).

In particular, for each month and for each point, a set of daily temperature values were generated by inverting the Gaussian density function (with mean equal to the mean temperature of that month and standard deviation obtained from table 1), from p=0.02 at the first day of the month, to p=0.98 at the last day of the month.

The potential snow melting for each month was then estimated as the sum of the potential melting in each day with mean temperature greater than zero, and as a weighted average of the following relations obtained from the “Handbook on the principles of Hydrology” (Donald M. Gray, 1973):

1) Melt Forest site = 2.286*T with T in °C and Melt in mm.
2) Melt Open site = 2.743*T+12.192 with T in °C and Melt in mm.

The two relations were considered for our case study area in the proportion 1) Melt Forest site =75% and 2) Melt Open site=25%. Results are presented in table 2. Melting is set to zero for mean monthly temperature lower than -1 °C.

Mean Monthly Temperature (°C)	Standard Deviation (°C)	Mean monthly temperature considering only values >0 °C (°C)	Melting Open Site (mm/day)	Melting Forest Site (mm/day)	Weighted Melting (mm/day)
0	2.4	0.9	14.8	2.2	3.5
1	2.8	1.7	16.8	3.9	7.1
2	3.3	2.5	19.1	5.8	9.1
3	3.1	3.3	21.1	7.4	10.9
4	2.5	4.0	23.3	9.2	12.8
5	2.6	5.0	26.0	11.5	15.1
6	2.7	6.0	28.7	13.7	17.4
7	2.8	7.0	31.4	16.0	19.9
8	2.9	8.0	34.1	18.3	22.3
9	2.8	9.0	36.9	20.6	24.7
10	2.6	10.0	39.6	22.9	27.1
11	2.5	11.0	42.4	25.1	29.5
12	2.6	12.0	45.1	27.4	31.9
13	2.6	13.0	47.9	29.7	34.3
14	2.3	14.0	50.6	32.0	36.7
15	2.5	15.0	53.3	34.3	39.1
16	2.7	16.0	56.1	36.6	41.5
17	2.2	17.0	58.8	38.9	43.9
18	2.3	18.0	61.6	41.1	46.3
19	2.1	19.0	64.3	43.4	48.7
20	2.0	20.0	67.1	45.7	51.1
21	2.0	21.0	69.8	48.0	53.5
22	2.0	22.0	72.5	50.3	55.9
23	2.0	23.0	75.3	52.6	58.3
24	2.0	24.0	78.0	54.9	60.7
25	2.0	25.0	80.8	57.2	63.1
26	2.0	26.0	83.5	59.4	65.5
27	2.0	27.0	86.3	61.7	67.9
28	2.0	28.0	89.0	64.0	70.3

Table 2. Potential snow melting (last column) as a function of monthly mean temperature (first column).

The snowpack (in terms of snow water equivalent) at the last day of each month (t_{end}) (time step = 1 month) has been modelled as follows:

$$SWE(t_{end}) = \max(0;\ SWE((t-1)_{end}) + Snow(t) - Potential\ \ Melting(t))$$

where Snow(t) is obtained multiplying the precipitation of month t by the frequency of days with T<1°C in the month (see table 3).

To test the procedure, in this explorative analysis the SWE of the basin has been estimated as weighted average of the different altitudinal belts, assigning to each elevation belt a mean temperature value based on the mean lapse rate of the area.
Being the results very promising, in future applications the high resolution of the data sets will be much more exploited.

Mean Monthly Temperature	Standard deviation of daily temperature	Frequency of days with T<1°C
-7.0	3.7	100%
-6.0	3.7	97%
-5.0	2.9	97%
-4.0	2.9	97%
-3.0	2.4	93%
-2.0	2.8	87%
-1.0	2.3	80%
0.0	2.4	67%
1.0	2.8	50%
2.0	3.3	37%
3.0	3.1	27%
4.0	2.5	10%
5.0	2.6	7%
6.0	2.7	3%
7.0	2.8	0%
8.0	2.9	0%
9.0	2.8	0%
10.0	2.6	0%
11.0	2.5	0%
12.0	2.6	0%

Table 3. Frequency of days with T<1°C as a function of mean monthly temperature.

2.2 Productivity model calibration

The potential productivity of the plant has been defined as follows:

$$P(t) = K \cdot \left(\frac{A \cdot P(t-1)}{K} + MAX\left\{0; B(T(t)) \cdot \left[\Pr(t) + SWE\left((t-1)_{end}\right) - SWE(t_{end})\right] - C(T(t))\right\} \right)$$

P is the estimated plant productivity;
Pr is the precipitation;
K has been obtained, for each of the 4 plants (there is one K coefficient per sub-catchment, i.e. one per plant), as the product between the area of the sub-catchment subtended by the plant and the energetic coefficient of the plant itself;
A=0.56 multiplied by the productivity of the previous month takes into account the delay in the runoff due to natural water storage;
B and C are coefficients dependent by temperature (see figure 1) and are the same for the different catchments. In this model the water loss for evaporation is assumed as a linear function of temperature (the term $C(T(t))$).
Once P(t) is estimated, the minimum between P(t) and the maximum theoretical potential productivity of the plant is considered.

The 1975-2010 period with available productivity data was divided into two sub-periods: 1975-1995 for the model calibration, and 1996-2010 for the model validation.

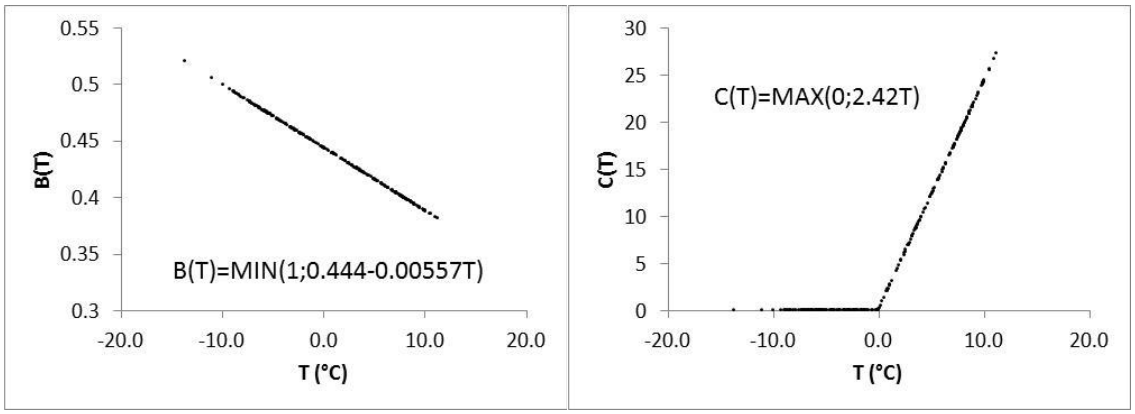

Figure 1. Coefficients B and C vs temperature.

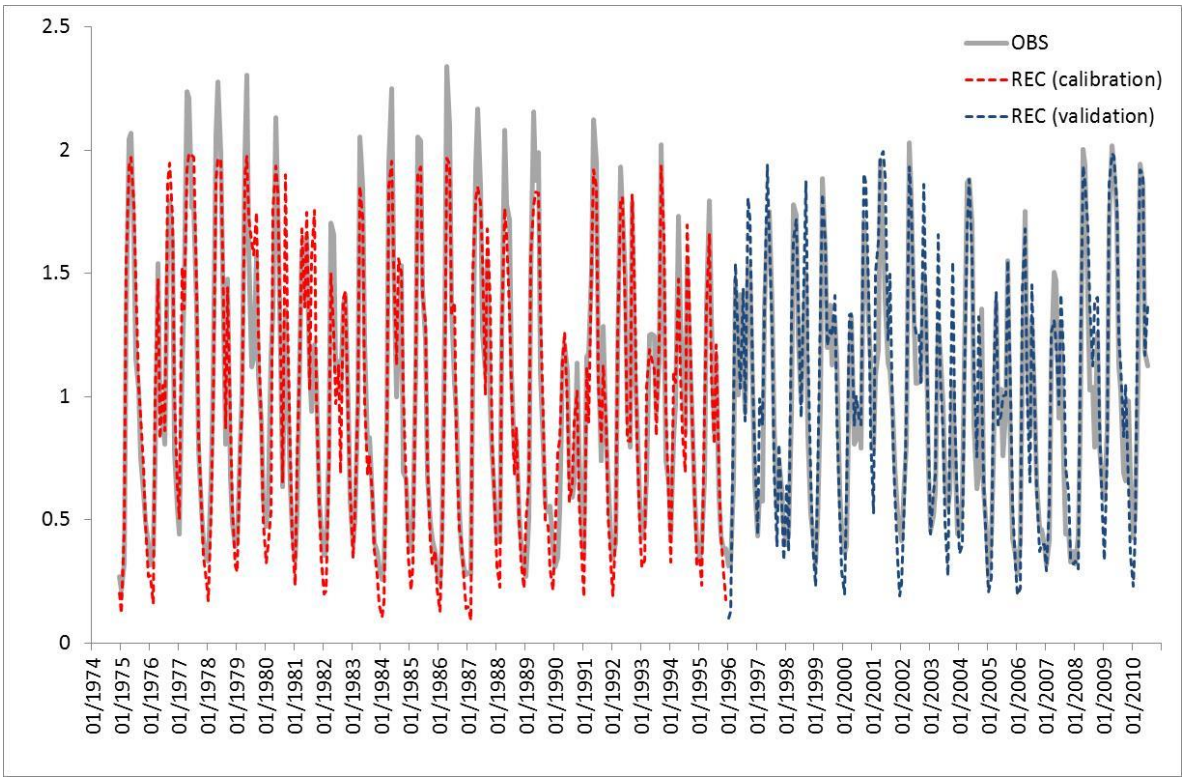

Figure 2. Comparison between the observed cumulative productivity of the 4 plants (grey line) and the simulated productivity (red line in the calibration period and blue line in the validation period).

Figures 2 and 3 show the comparison between the observed cumulative productivity of the 4 plants and the simulated productivity obtained using the above discussed relationship (data are expressed in terms of ratios with respect to the mean productivity of the plants).

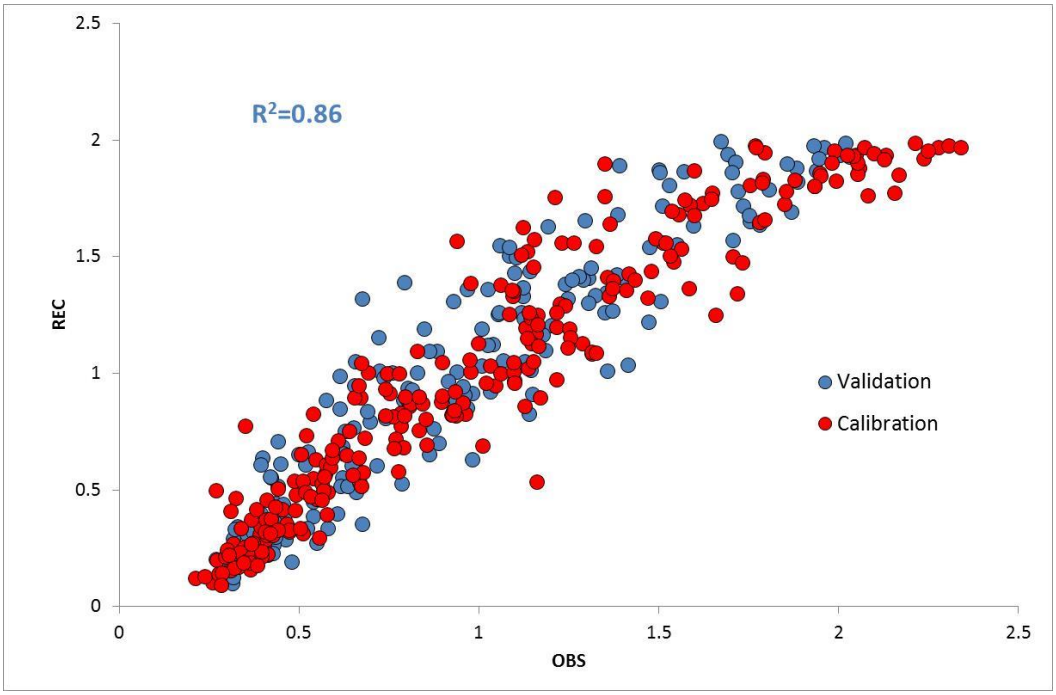

Figure 3. scatter plot of the simulated productivity versus observed cumulative productivity of the 4 plants (red dots: calibration period, blue dots: validation period). The squared correlation coefficient estimated over the validation period is indicated too.

The productivity data used for the calibration of the model were obtained by summing to the productivity of the plants the eventual volume of water storable into the tanks located upstream of each plant. In the modelled data the possibility of water storage was not included and this explains the lower upper limit of the reconstructed productivity with respect to the observed one (figure 3).

3. Future productivity of the hydropower plant under climate change

Once the model has been calibrated and validated, it has been used to simulate the future potential productivity of the 4 plants starting from the temperature and precipitation data sets for the period 2001-2100 obtained downscaling four RCMs model outputs from the ENSEMBLES project under an A1B scenario.

3.1. 2001-2100 high resolution temperature and precipitation data sets

Four RCMs were taken into account: KNMI-ECHAM5, SMHI-ECHAM5, SMHI-BCM and SMHI-Had. We considered the historical run of the models forced by GCM and their future projections under the A1B scenario.

To downscale RCMs to the high resolution of past reconstruction, each grid point monthly series of each model output (from the historical run to the future projection) has been converted into an anomaly record with respect to its 1961-1990 mean annual cycle (multiplicative anomalies for precipitation. This conversion was obtained by dividing each value by the corresponding 1961-1990 monthly normal). These series were then interpolated (as we already did with the historical homogenized stations' series) onto the same nodes of the 1-km^2 resolution temperature and precipitation climatologies produced in deliverable 6.4.

Finally, they were converted into absolute monthly temperature and precipitation by adding to (multiplying for precipitation) each series the climate normal of the corresponding 1-km^2 grid-cell. In this way we obtained, for each model, a high resolution grid of bias-corrected monthly temperature and precipitation series for the 1961-2100 period.

Figures 4-7 show the temperature and precipitation evolution for the next 100-year period.

Mean temperatures for the different models are comprised in a range of 0.8°C in the first 25-year; in the last 25-year period (figure 4) this range increases to 1.4°C, highlighting some differences in the long term trend of the different models. The good agreement between KNMI-ECHAM and SMHI-ECHAM suggests that the GCM is the driving component.

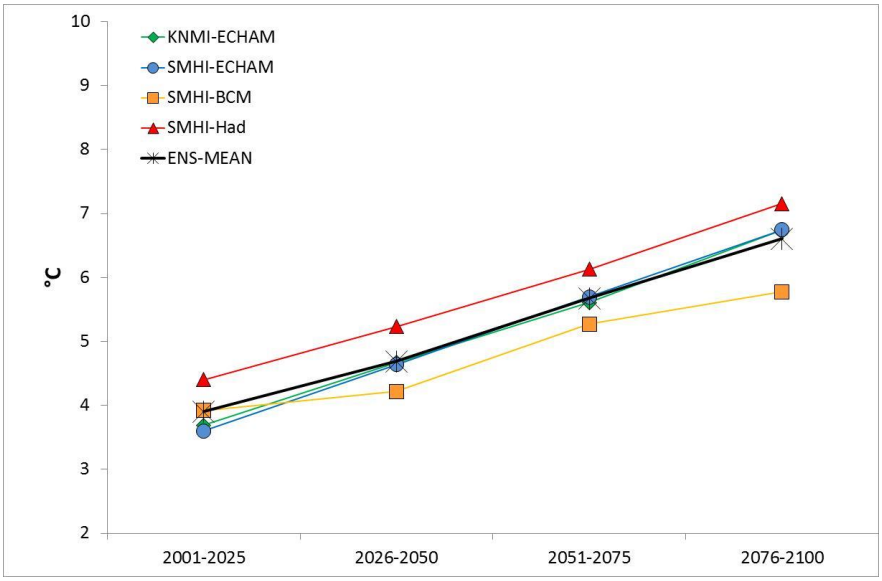

Figure 4. Mean temperature evolution in the 2001-2100 period for the four RCMs' outputs and their ensemble mean

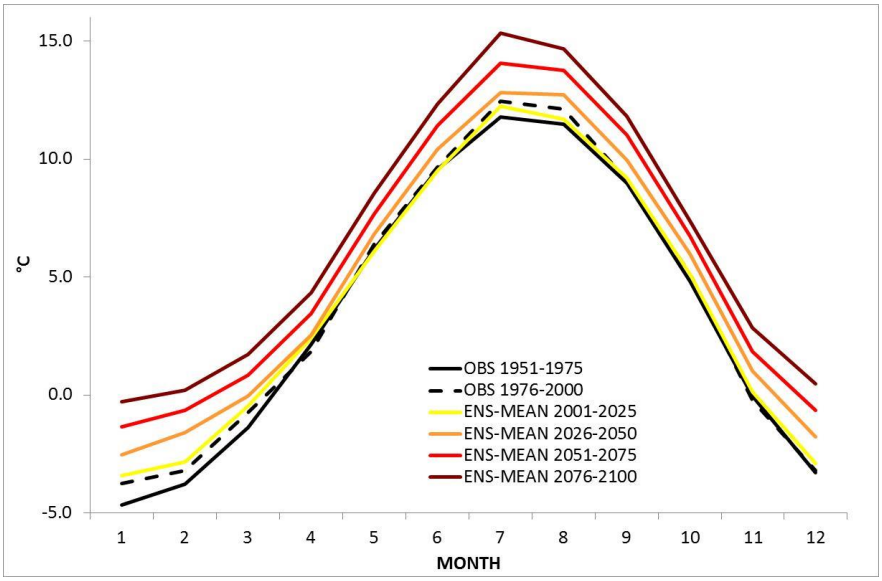

Figure 5. Evolution of the temperature annual cycle in the 2001-2100 period for the ensemble mean of the four RCMs' outputs.

As far as precipitation is concerned, all model but SMHI-Had agree in a reduction of the total annual amount (figure 6), particularly relevant in the last 25-year period. SMHI-Had, on the contrary, foresees a progressive increase in total precipitation, in contradiction with the other models. This should be attributed to the GCM forcing SMHIRC, being the results of the same RCM forced by other GCMs completely different.

From figure 7 it is evident that the precipitation decrease is concentrated in late spring and summer, on the contrary a precipitation increase is evident in late winter and early spring (figure 7).

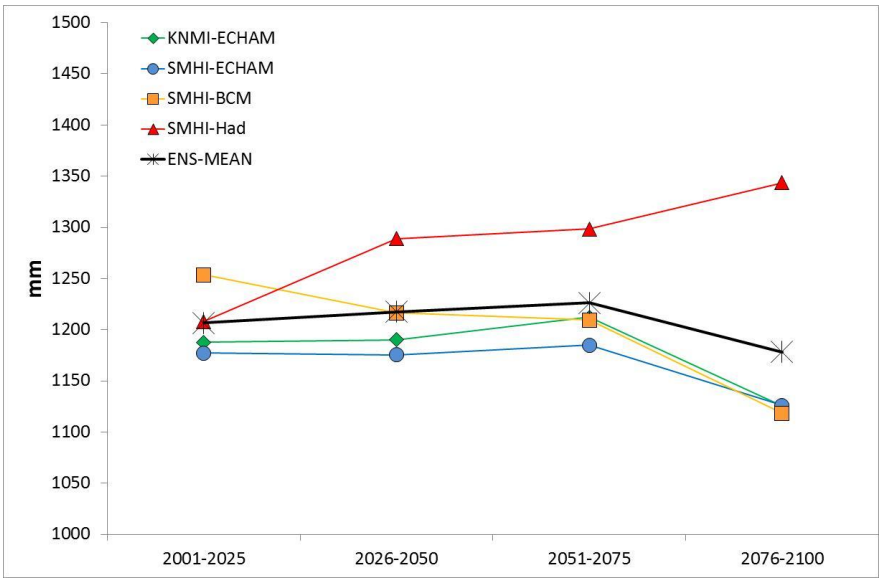

Figure 6. Total mean annual precipitation evolution in the 2001-2100 period for the four RCMs' outputs and their ensemble mean

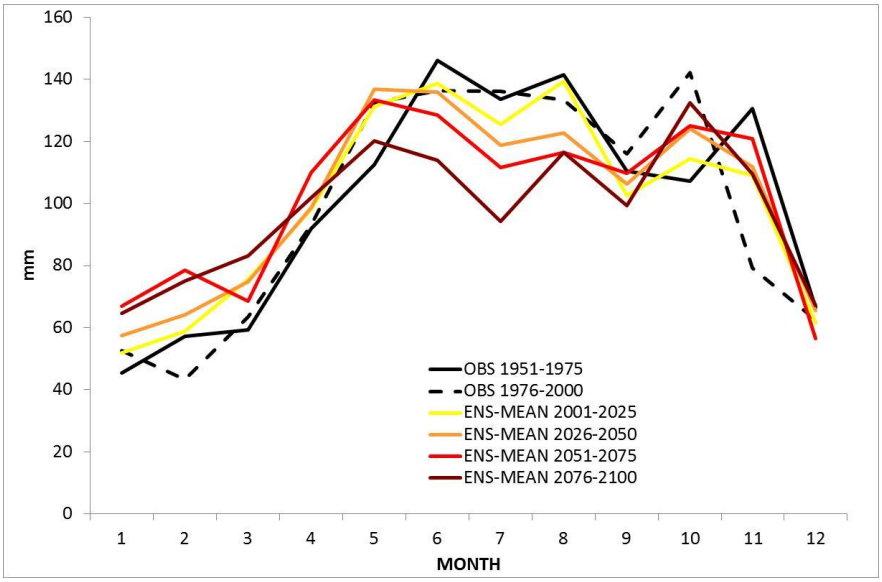

Figure 7. Evolution of the precipitation annual cycle in the 2001-2100 period for the ensemble mean of the four RCMs' outputs.

Figures 8 and 9 show the SWE evolution for the next 100-year period. It is evident a significant reduction of the SWE mostly due to the reduction of solid precipitation fraction during winter season, linked to the temperature increase.

The lower storage of snow during winter season and the decrease in summer precipitation will significantly affect the water availability for hydropower production and its distribution through the year. In fact, all models, but SMHI-Had, foresee a reduction of about 10% of the plant productivity at the end of the XXI century (figures 10 and 11).

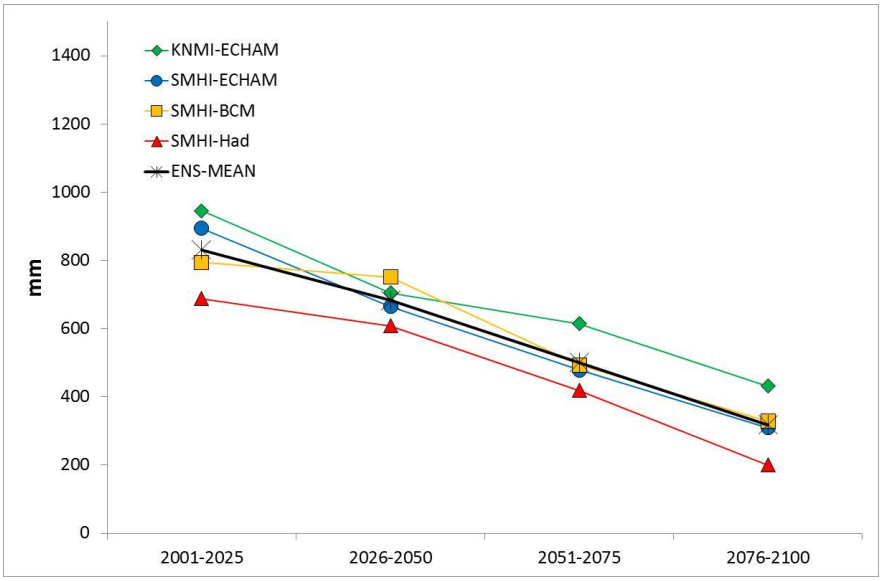

Figure 8. Total mean annual SWE evolution in the 2001-2100 period for the four RCMs' outputs and their ensemble mean

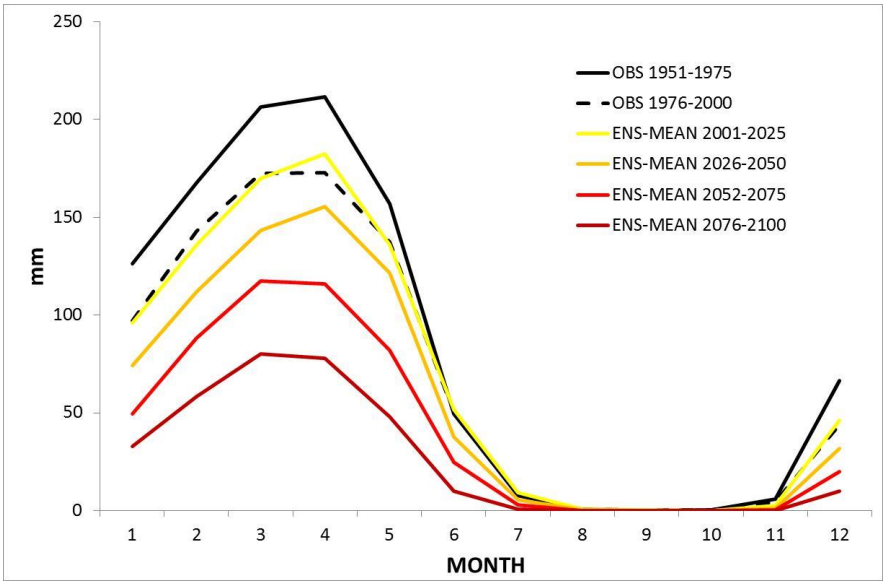

Figure 9. Evolution of the SWE annual cycle in the 2001-2100 period for the ensemble mean of the four RCMs' outputs.

The decrease is particularly evident in summer, due to a significant reduction in mean precipitation. On the contrary, there is an increase in the winter productivity due to both an increase in total winter precipitation but also to an increase in its liquid component, to the detriment of a lower productivity in spring due to the lower storage of solid precipitation in winter season.

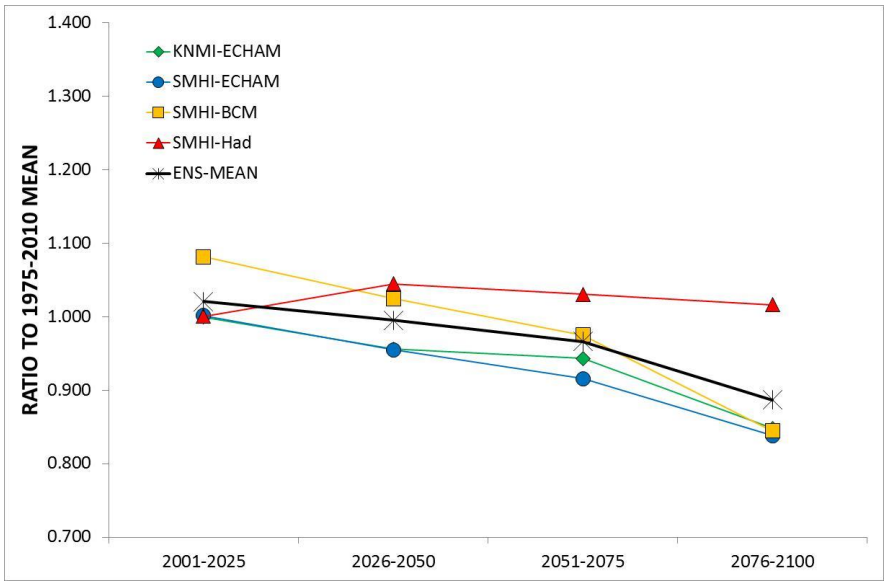

Figure 10. Total mean annual productivity evolution in the 2001-2100 period for the four RCMs' outputs and their ensemble mean

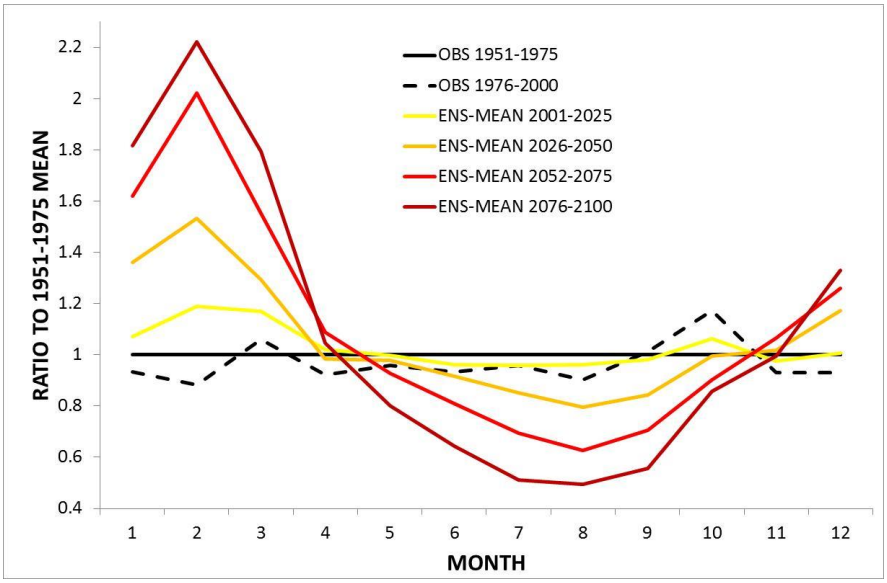

Figure 11. Evolution of the productivity annual cycle in the 2001-2100 period for the ensemble mean of the four RCMs' outputs (relative to the 1951-1975 period).

To highlight the role of precipitation alone affecting plant productivity, we replicated the same 25-year sequence of past 1975-2000 observed temperature in the four future 25-year sub-periods and repeated the analysis. In this way, the role of temperature changes from one sub-period to the others is eliminated, and only the effect of precipitation changes is highlighted.

Figures 12 and 13 show the result of this analysis. It is evident a light reduction in the last 25-year period (2075-2100), where the only clear precipitation decrease is observed in all models but SMHI-Had, mainly due to summer and autumn period.

This demonstrates that the most relevant climate-change-impact affecting future hydropower productivity is foreseen to be the one linked to temperature (affecting both snow melting and the fraction of solid and liquid precipitation, i.e. snow storage) and not that linked to precipitation.

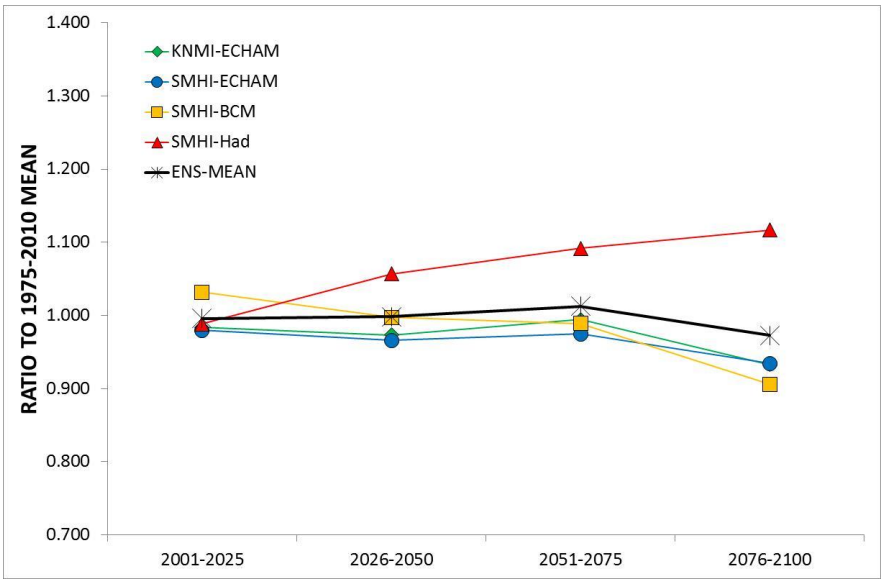

Figure 12. The same as figure 10, but replicating the past 1975-2000 temperature sequence in the future four 25-year periods (i.e. excluding the temperature changes)

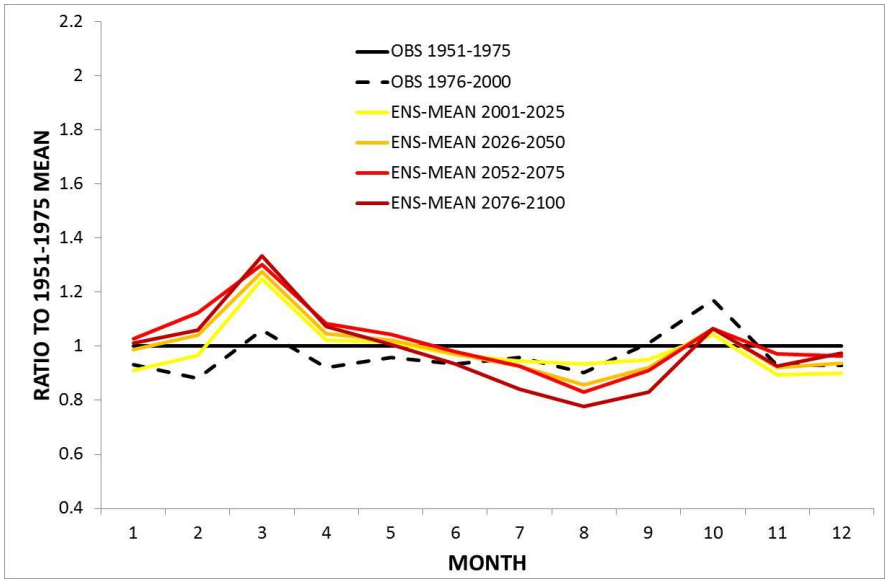

Figure 13. The same as figure 11, but replicating the past 1975-2000 temperature sequence in the future four 25-year periods (i.e. excluding the temperature changes)

References

Donald M. Gray, 1973, “Handbook on the principles of hydrology”, Water Information Center – Port Washington, Canada

Links to concrete results:

http://www.eclise-project.eu/

http://www.isac.cnr.it/ECLISE-project.html

References to activity meetings:

The objectives of these maps have been presented at the ECLISE Kick-off meeting (De Bilt - 09 March 2011.

The methods and results have been presented at the First ECLISE meeting (Norrkhoping - 6-7 March 2012).